

Internal energy change and activation energy effects on Casson fluid

Cite as: AIP Advances **10**, 025009 (2020); <https://doi.org/10.1063/1.5140349>

Submitted: 26 November 2019 • Accepted: 17 January 2020 • Published Online: 05 February 2020

T. Salahuddin, Nazim Siddique, Maryam Arshad, et al.

COLLECTIONS

Paper published as part of the special topic on [Mathematical Physics](#)



View Online



Export Citation



CrossMark

ARTICLES YOU MAY BE INTERESTED IN

[Heat and mass transfer together with hybrid nanofluid flow over a rotating disk](#)

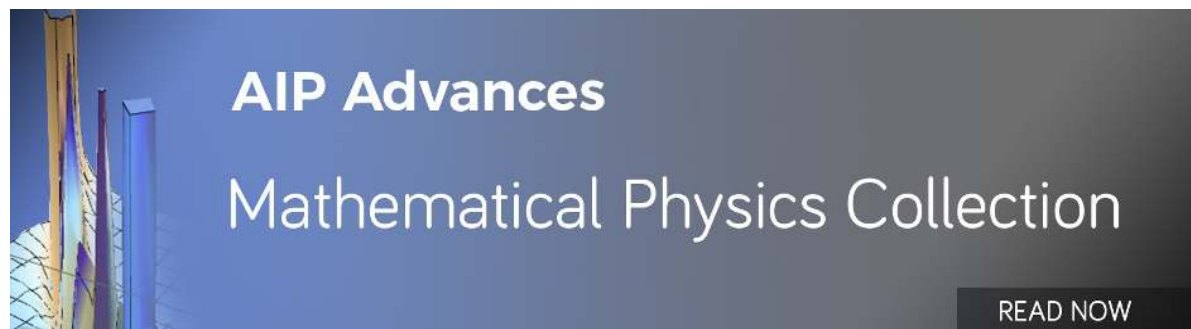
AIP Advances **10**, 055317 (2020); <https://doi.org/10.1063/5.0010181>

[Darcy-Forchheimer flow of Maxwell nanofluid flow with nonlinear thermal radiation and activation energy](#)

AIP Advances **8**, 035102 (2018); <https://doi.org/10.1063/1.5019218>

[Entropy generation in MHD Maxwell nanofluid flow with variable thermal conductivity, thermal radiation, slip conditions, and heat source](#)

AIP Advances **10**, 015038 (2020); <https://doi.org/10.1063/1.5129569>




Internal energy change and activation energy effects on Casson fluid

Cite as: AIP Advances 10, 025009 (2020); doi: 10.1063/1.5140349

Submitted: 26 November 2019 • Accepted: 17 January 2020 •

Published Online: 5 February 2020



T. Salahuddin,¹ Nazim Siddique,^{1,a)} Maryam Arshad,¹ and I. Tlili² 

AFFILIATIONS

¹Department of Mathematics, Mirpur University of Science and Technology (MUST), Mirpur 10250, AJK, Pakistan

²Department of Management of Science and Technology Development, Ton Duc Thang University, 758307 Ho Chi Minh City, Vietnam

^{a)} Author to whom correspondence should be addressed: nazimsiddique11@gmail.com

ABSTRACT

This paper examines the steady-state momentum heat and mass transfer flow of a Casson fluid flow in the existence of a pre-exponential factor. The velocity of the fluid over a vertical stretched pin changes linearly with the axial distance when a Casson model is supposed for the viscosity. A similarity transformation eases the Navier–Stokes partial differential equations that are converted into ordinary differential equations and solved numerically for concentration, velocity, and temperature fields. Moreover, viscosity and conductivity are assumed to be dependent on the temperature profile. Results are discussed for two boundary conditions of the pin, while diffusivity is dependent on concentration. A reaction in the form of a pre-exponential factor is taken on the surface of the pin. Parameters such as the mixed convection parameter, viscosity parameter, and viscoelastic parameter are considered for the control of the flow field. In addition, the internal energy change and the Prandtl number are found to examine the temperature field inside the stretched pin, while the Schmidt number, temperature relative parameter, concentration buoyancy parameter, activation energy parameter, and chemical reaction parameter control the concentration field.

© 2020 Author(s). All article content, except where otherwise noted, is licensed under a Creative Commons Attribution (CC BY) license (<http://creativecommons.org/licenses/by/4.0/>). <https://doi.org/10.1063/1.5140349>

INTRODUCTION

In a chemical system, the amount of energy required to control the atoms or molecules during a chemical reaction is known as the pre-exponential factor. This term was first introduced in 1889 by Svante Arrhenius, a Swedish scientist, and it is measured in kJ/mol. There is no pre-exponential factor in several elements and compounds when they react with each other, while some atoms or molecules give out a specific amount of energy in the form of activation. Generally, a pre-exponential factor is the unraveling boundary between two states of energy. Whenever this boundary of energy is crossed, a chemical reaction will be started. A chemical reaction proceeds at an equitable rate if there exists a specific number of molecules or atoms with activation energy less than or equal to translational energy. In various fields such as oil reservoirs and chemical and geothermal engineering, a part of the pre-exponential factor is usually applicable experimentally due to the chemical reaction involved in the system. There are several publications in fluid

mechanics which explain the physical features of the pre-exponential factor along with chemical reaction. The influence of heat generation and energy activation in 2D free convective flow over a permissible medium was discussed by Patil *et al.*¹ Hayat *et al.*² elaborated the chemical reaction effect on viscoelastic fluid flow in the presence of mass and heat transfer. They elaborated the homotopy analysis method for the series solution and checked the rate of convergence of series solution. Maleque³ studied the impact of change in internal energy and heat absorption on MHD boundary layer mass and heat transfer flow with energy activation and chemical reaction. Awad *et al.*⁴ scrutinized the impact of energy activation along with chemical reaction for unsteady revolving fluid flow over a stretchable surface. Shafique *et al.*⁵ examined the spinning flow of non-viscous fluid over an expanding surface under the impact of binary chemical reaction along with energy activation. Hsiao⁶ took nanofluid and explained non-Newtonian flow with the existence of activation energy and gave a theoretical framework of the promotion of economic efficiency improvement in the manufacturing process. Lu *et al.*⁷

deliberated the impact of chemical reaction and activation energy on the MHD revolving flow of viscoelastic fluid with a non-Fourier heat flux model. Hamid *et al.*⁸ calculated the effects of binary chemical reaction along with energy activation on the non-Newtonian fluid flow produced by a stretching cylinder. Dhlamini *et al.*⁹ presented a theoretical work of mixed convection flow over an infinite surface by assuming mutual effects of binary chemical reaction along with energy activation. Majeed *et al.*¹⁰ studied the model of viscoelastic flow and found the solution by using the Lobatto (IIIA) scheme and checked the influence of energy activation and chemical reaction upon different distributions. Khan *et al.*¹¹ considered the influence of activation energy and investigated the MHD stagnation point flow of viscoelastic fluid toward an extended surface. Ijaz and Ayub¹² explored a model of the Maxwell nanofluid with activation energy and flow being produced by stretching of an inclined cylinder.

Heat transfer plays a vital role owing to their extensive uses in biomedicine, plasma physics, oceanography, metrology, physical chemistry, and many others. Many engineering progressions such as distillation of liquid, heat exchange, refrigeration of an atomic controller, etc., are main applications of heat transfer. In fluid mechanics, it was examined that viscosity creates resistance to fluid motion, and during this procedure, some amount of mechanical energy is converted into heat energy. This procedure is called change in internal energy. Brinkman¹³ was the person who first analyzed this fact in his research paper. He analyzed the effect of change in internal energy in a capillary flow. Wei and Luo¹⁴ included the change in internal energy effect in the temperature equation and presented the power law model. Jambal *et al.*¹⁵ scrutinized the change in internal energy effect for viscoelastic fluid in a circular channel with step change ambient temperature. Kairi and Murthy¹⁶ illustrated the change in internal energy effect on natural convection mass and heat transfer over a vertical cone in an absorbent medium embedded with viscoelastic fluid. El-Aziz¹⁷ discussed the non-Newtonian fluid with the change in internal energy and variable viscosity along a semi-infinite vertical elongating surface. Saleem and Nadeem¹⁸ presented a framework of the change in internal energy and slip effect over a rotating cone. Sheri and Shamshuddin MD¹⁹ conferred the mass and heat transfer on the MHD flow of micro-polar fluid and the effects of the change in internal energy along with chemical reaction. Hussain *et al.*²⁰ discussed MHD Sisko fluid flow due to an expanding cylinder under the effects of variable thermal conductivity and change in internal energy. Salahuddin *et al.*²¹ scrutinized the effect of change in internal energy on MHD tangent hyperbolic fluid flow with convective boundary constraints over a nonlinear stretched surface. Hussain *et al.*²² presented cumulative effects of Joule heating and change in internal energy on MHD Sisko fluid flow over a stretchable cylinder in existence of nanoparticles.

The phenomenon that designates the capacity of a material to transfer heat is known as thermal conductivity. It plays an important role in cooling of materials. However, it can be observed experimentally that thermal conductivity is affected by thickness and temperature especially when existence of temperature differences is very large. Due to this fact, many scholars paid attention on the influence of temperature dependent thermal conductivity on a stretching surface. Elbarbary *et al.*²³ discussed the influence of variable thermo-physical properties on micro-polar fluid flow over a moving porous surface with radiation. Saleem²⁴ studied viscoelastic fluid flow over

an elongated medium with variable viscosity and thermal conductivity. Ahmad *et al.*²⁵ scrutinized variable thermal conductivity on boundary layer flow passing through an extended plate. Hayat *et al.*²⁶ studied 3-D unsteady mixed convection flow in the appearance of variable thermal conductivity. Hashim *et al.*²⁷ discussed the impact of variable thermal conductivity on mixed convection flow of the Williamson fluid with the incidence of nano-particles.

Viscosity is the fundamental property of fluid that resists the movement of liquid and gas molecules. The variation in different factors such as pressure, shear rate, and temperature causes variation in fluid viscosity. The quality of nylon and rayon production, paper and textile manufacturing, plastic extrusion, and many other engineering processes depend upon these factors. Therefore, it is important to assume that viscosity will be dependent upon temperature. Pantokratoras²⁸ conferred the influence of variable viscosity on MHD flow passing through an extended surface. Tsai *et al.*²⁹ studied boundary layer flow passing through an unceasing moving absorbent surface with temperature dependent thermo-physical properties. Malik *et al.*³⁰ conferred the impact of variable viscosity on boundary layer flow of viscoelastic fluid flow due to a horizontally stretched cylinder. Malik *et al.*³¹ initiated a numerical clarification for viscoelastic fluid flow toward a stretchable surface and found the solution by using the Keller box method. Umavathi *et al.*³² considered thermal conductivity and viscosity as exponential functions of temperature and gave an analysis method to obtain the flow of viscous fluid. Akinbobola and Okoya³³ scrutinized the impact of variable thermal conductivity and viscosity on second grade fluid flow past a stretchable surface in the presence of a heat source/sink.

The conjugate influence of heat and mass transfer is of particular prominence in industrial and engineering processes. Chemical species and thermal diffusion are main causes for such enlargement in construction and help in various technological innovations such as manufacturing of polymer and ceramics, nuclear safety, improved oil recovery, paper making and design machines, food processing, fog creation to diffusion, underground energy transport, and many others. Therefore, in the last few years, many researchers have shown great interest in influence of chemical species on the transport of mass in fluid flows. Muthucumaraswamy^{34,35} studied the impact of variable diffusivity flow passing through a moving vertical plate and solved the model by using Laplace transformation. Rajesh and Varma³⁶ scrutinized the impact of mass diffusion on MHD flow passing through an absorbent medium. Jia *et al.*³⁷ discussed the 1D advection-diffusion equation for two different cases: (i) when mass diffusion is constant and flow velocity is variable and (ii) when both velocity of flow and diffusion are variables. They obtained an analytical solution and made a comparison between the two different situations. Li *et al.*³⁸ presented a model in which they discussed the impact of variable thermo-physical properties on nonlinear transitory responses of comprehensive diffusion-thermo elasticity. Sheng *et al.*³⁹ discussed experimentally the mechanism of thermal diffusion for moving particles in a vibrated granular system. Qureshi *et al.*⁴⁰ investigated the impact of mass diffusion and thermal conductivity as functions of concentration and temperature on transportation of mass and heat in the flow of viscous fluid. Khan *et al.*⁴¹ conferred the impact of thermal diffusion and conductivity in Maxwell fluid flow passing through an expanded surface in the presence of nanoparticles. Some latest publications related to this work are mentioned in Refs. 42–45.

A cautious view of the current literature reveals that nobody has deliberated the influence of thermo-physical properties along with the pre-exponential factor and internal energy change for the Casson fluid around a vertical moving pin. Due to this fact, the current analysis has novelty and studied the demeanor of concentration and temperature dependent thermo-physical properties in the presence of the pre-exponential factor for the fluid around a vertical moving pin. Moreover, the impact of internal energy change is taken into consideration in the energy equation. The governing system of PDEs is reduced into a system of non-dimensional ODEs with the help of apposite similarity transformations. An appropriate piece of Matlab software (Bvp4c) is used for the purpose of numerical solutions. The graphical influence of several parameters is inspected for momentum, energy, and concentration fields. Tables containing the Nusselt number, skin friction, and Sherwood numbers are presented and well argued.

PROBLEM ANALYSIS

Let us consider steady mixed convection and in-compressible boundary layer transport of viscoelastic fluid flow through a vertical moving pin (as shown in Fig. 1). The magnitude of the moving pin is assumed to be thin, and its thickness is lower than the boundary layer thickness. The effect of transverse curvature is an important factor, but the body forces and gradient of pressure are neglected due to the small thickness of the pin. Let us suppose that the pin is moving with a uniform velocity u_w ; in the mainstream, the uniform velocity is u_∞ . The function $r = R(x) = \sqrt{v_c x / U}$ describes the shape of the vertically thin pin in which $U = u_\infty + u_w$ represents the combined velocity of the mainstream and pin. Moreover, we assume that T_∞ and T_w are ambient fluid and funnel surface temperatures, respectively, which are constants, where $T_\infty < T_w$. The impacts are encompassed in our model.

Variable thermo-physical properties

Viscosity of fluid is changed when the temperature difference is very large. We assume an inverse relation between viscosity and the

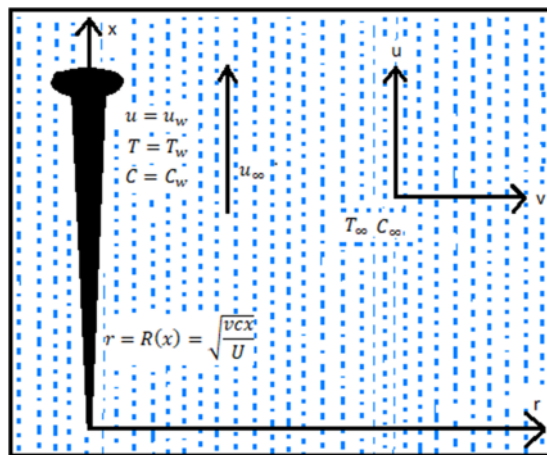


FIG. 1. Flow geometry and the coordinate system.

linear function of temperature, i.e.,

$$\mu = \frac{\mu_0}{(\omega(T - T_\infty) + 1)} \text{ or } \mu = \frac{1}{\sigma(T - T_r)}, \tag{1}$$

where $T_r = T_\infty - \omega^{-1}$ and $\sigma = \omega\mu_0^{-1}$ are constants, and μ_0 represents the ambient dynamic viscosity. The fluid thermal property ω and the reference state of fluid affected the performance of these constants. Usually, for gases, we take σ as positive, and for liquids, we take σ as negative.

The impact of temperature dependent thermal conductivity comprises in the energy equation. We assume a direct relation between thermal conductivity and temperature, i.e.,

$$K(T) = K_\infty \left(1 + \varepsilon \left(\frac{T - T_\infty}{T_w - T_\infty} \right) \right), \tag{2}$$

where the temperature parameter ε is very small. If $\varepsilon = 0$, then thermal conductivity does not show any variation.

Similarly, in the concentration equation, we encompass concentration dependent mass diffusion. There are a large number of analogies that exist between heat and mass transfer, and one can measure that the mass diffusion D and concentration C are linearly dependent to each other,

$$D(C) = D_\infty \left(1 + \varepsilon_1 \left(\frac{C - C_\infty}{C_w - C_\infty} \right) \right), \tag{3}$$

where C_w is the constant concentration at the barrier of the pin, and C_∞ is the ambient concentration. The concentration parameter ε_1 is very small. Equation (3) indicates that no variation exists in mass diffusion if $\varepsilon_1 = 0$.

Pre-exponential factor and change in internal energy

It can be seen that the pre-exponential factor is affected by the rate of biochemical reaction. Recently, most of the publication on the influence of the pre-exponential factor shows the importance of this fact. Motivated from these publications, we include the Arrhenius pre-exponential factor law (see Ref. 3) in the concentration equation, i.e.,

$$K^* = k_r^2 \left(\frac{T}{T_w} \right)^n \exp\left(\frac{-Ea}{kT} \right) (C - C_\infty),$$

where K^* represents the chemical reaction rate, and k is the Boltzmann constant having a value $\frac{8.61}{10^5}$ eV/K. The physical constant k connects the energy of individual particles and combined particle levels. k_r^2 is the constant rate of chemical reaction, and Ea is the energy activation.

In the energy equation, we include the impact of internal energy change, i.e.,

$$\text{Internal energy change} = \mu(1 + \gamma^{-1})(\partial_r u)^2.$$

With the help of this assumption, the non-dimensional form of governing equations after raising Boussinesq and boundary layer approximations is as follows:

$$\partial_x(ru) + \partial_r(rv) = 0, \tag{4}$$

$$u\partial_x u + v\partial_r u = (1 + \gamma^{-1}) \left(\frac{r\partial_r \mu \partial_x u + \mu \partial_r u + \mu r \partial_r^2 u}{r\rho} \right) + g((C - C_\infty)\beta_C + (T - T_\infty)\beta_T), \quad (5)$$

$$u\partial_x T + v\partial_r T = (K\partial_r T + r\partial_r K\partial_r T + rK\partial_r^2 T) + \mu(1 + \gamma^{-1})(\partial_r u)^2, \quad (6)$$

$$u\partial_x C + v\partial_r C = \left(\frac{rD\partial_r^2 C + D\partial_r C + r\partial_r D\partial_r C}{r} \right) - k_r^2 \left(\frac{T}{T_w} \right)^n \exp\left(\frac{-Ea}{kT}\right)(C - C_\infty), \quad (7)$$

along with boundary constraints

$$v = 0, \quad u = u_w, \quad T = T_w, \quad C = C_w \quad \text{when } r = R(x), \quad (8)$$

$$u \rightarrow u_\infty, \quad T \rightarrow T_\infty, \quad C \rightarrow C_\infty \quad \text{when } r \rightarrow \infty.$$

Here (u, v) signifies the component of velocity along axial x and radial r directions, respectively. The concentration and temperature of fluid is denoted by C and T, respectively. The coefficients of concentration and thermal expansions are denoted by β_C and β_T , respectively. μ , K, and D are defined in Eqs. (1)–(3). The exponential fitted rate is denoted by n having a range (−1, 1), and the density of fluid is denoted by ρ .

We consider an opposite similarity transformation $\eta = \frac{r^2 U}{xv_0}$ and propose the non-dimensional functions $\varphi(\eta)$, $\theta(\eta)$, and $f(\eta)$ as

$$\varphi(\eta) = \frac{C - C_\infty}{C_w - C_\infty}, \quad \theta(\eta) = \frac{T - T_\infty}{T_w - T_\infty}, \quad f(\eta) = \frac{\zeta}{xv_0}, \quad (9)$$

where ζ is a stream function, which can be demarcated as

$$u = \frac{1}{r} \partial_r \zeta \quad \text{and} \quad v = -\frac{1}{r} \partial_x \zeta, \quad (10)$$

in which the in-compressibility condition given in Eq. (4) is fulfilled identically, and Eqs. (5)–(7) give the following nonlinear dimensionless form:

$$f''f + 2 \frac{\eta \theta' (1 + \gamma^{-1}) f''}{\theta_r} + 2 \frac{(1 + \gamma^{-1})(\theta_r + \theta)(\eta f'''' + f'')}{\theta_r} + \frac{(N\varphi + \theta)\lambda}{4} = 0, \quad (11)$$

$$2\varepsilon\eta\theta'^2 + (\theta\varepsilon + 1)\theta' + (\theta\varepsilon + 1)(2\eta\theta'' + \theta') + 8 \frac{(1 + \gamma^{-1})(\theta_r + \theta)}{\theta_r} \eta Ec Pr f''^2 + Pr f \theta' = 0, \quad (12)$$

$$2\varepsilon_1 \eta \varphi'^2 + 2(\varphi\varepsilon_1 + 1)\varphi' + 2\eta(\varphi\varepsilon_1 + 1)\varphi'' + Sc\varphi'f - \sigma_m Sc(1 + \theta\delta)^n \exp\left(\frac{-E}{1 + \theta\delta}\right) = 0, \quad (13)$$

along boundary restrictions

$$f = \frac{\alpha}{2}m, \quad f' = \frac{\alpha}{2}, \quad \theta = 1, \quad \varphi = 1 \quad \text{when } \eta = m, \quad (14)$$

$$f' \rightarrow \frac{1 - \alpha}{2}, \quad \theta \rightarrow 0, \quad \varphi \rightarrow 0 \quad \text{when } \eta \rightarrow \infty.$$

Here $\alpha = \frac{u_w}{U}$ is the ratio between the velocity of the pin and the combined velocity of the mainstream and pin. Note that $\alpha = 0$ corresponds to the static pin in a Blasius flow (moving fluid), and $\alpha = 1$ indicates the moving pin in a Sakiadis flow (stationary fluid). Prime signifies the derivative with respect to η . Equations (11)–(13) include the non-dimensional mixed convection parameter λ , variable thickness parameter θ_r , Prandtl number Pr, Schmidt number Sc, temperature relative parameter δ , Eckert number Ec, concentration buoyancy parameter N, activation energy parameter E, and chemical reaction parameter σ_m , which are defined as follows:

$$\lambda = \frac{Gr_x}{Re_x^2}, \quad Pr = \frac{\mu_0 c_p}{K_\infty}, \quad \theta_r = \frac{-1}{\gamma(T_w - T_\infty)}, \quad Sc = \frac{v_0}{D_\infty}, \quad \delta = \frac{T_w - T_\infty}{T_\infty},$$

$$Ec = \frac{U^2}{(T_w - T_\infty)c_p}, \quad N = \frac{\beta_C(C_w - C_\infty)}{\beta_T(T_w - T_\infty)}, \quad E = \frac{Ea}{kT_\infty}, \quad \sigma_m = \frac{k_r^2 x}{2U}, \quad (15)$$

where $Gr_x = \frac{g\beta_T(T_w - T_\infty)x^3}{\nu_0}$ is the local Grashof number which gives the ratio between buoyancy and viscous forces.

The physical properties of fluid such as the Sherwood number Sh_x , Nusselt number Nu_x , and skin friction coefficient C_f are written as

$$Sh_x = \frac{xj_w}{D(C_w - C_\infty)}, \quad Nu_x = \frac{xq_w}{k(T_w - T_\infty)}, \quad C_f = \frac{\tau_w}{\rho U^2}, \quad (16)$$

where q_w represents the heat flux, j_w denotes the mass flux at the surface, and τ_w is the skin friction, which can be written as

$$j_w = -D\partial_r C|_{r=R(x)}, \quad q_w = -k\partial_r T|_{r=R(x)}, \quad \tau_w = \mu(1 + \gamma^{-1})(\partial_x v + \partial_r u), \quad (17)$$

and after imposing the transformation in Eq. (16), we obtained the following non-dimensional form:

$$\frac{Sh_x}{\sqrt{Re_x}} = -2\sqrt{m}\varphi'(m), \quad \frac{Nu_x}{\sqrt{Re_x}} = -2\sqrt{m}\theta'(m), \quad (18)$$

$$C_f\sqrt{Re_x} = 4(1 + \gamma^{-1})\left(\frac{\theta_r + \theta}{\theta_r}\right)\sqrt{mf''}.$$

Here, $Re_x = \frac{Ux}{\nu_0}$ represents the Reynolds number.

NUMERICAL SOLUTION

In this section, we describe the numerical solution for the governing problem, which is clarified via the Bvp4c technique. To achieve this, a Bvp4c scheme is betrothed to discretize the conservative 3rd and 2nd order equations into the 1st order form. For the purpose of residual solution, a finite point is used instead of infinity and adjusted based on initial guesses according to different parameters. Moreover, we create an error controller and mesh collection. The tolerance of relative errors has been set to 0.000 001. For perseverance of this technique, we revise higher orders [Eqs. (11)–(13)] into first order differential equations as follows:

$$f = y_1, \quad f' = y_2, \quad f'' = y_3,$$

$$f''' = -\frac{\left(2(1 + \gamma^{-1})\left(1 + \frac{1}{\theta_r}y_4 + \frac{\eta}{\theta_r}y_5\right)y_3 + y_1y_3 + \frac{1}{4}y_4 + \frac{1}{4}Ny_6\right)}{2(1 + \gamma^{-1})\left(1 + \frac{y_4}{\theta_r}\right)\eta}, \quad (19)$$

$$\theta = y_4, \quad \theta' = y_5,$$

$$\theta'' = -\frac{(2(1 + \epsilon y_4)y_5 + 2\epsilon\eta y_5^2 + \text{Pr} y_1 y_5 + 8(1 + \gamma^{-1})\left(1 + \frac{y_4}{\theta_r} \text{Pr} \text{Ec} y_3^2\right))}{2\eta(1 + \epsilon y(5))}, \tag{20}$$

$$\varphi = y_6, \quad \varphi' = y_7,$$

$$\varphi'' = -\frac{(2(1 + \epsilon_1 y_6)y_7 + 2\epsilon_1\eta y_7^2 + \text{Sc}(y_1 y_7 - \sigma_m(\delta y_4 + 1)^w \exp\left(\frac{-E}{\delta y_4 + 1}\right)))}{2\eta(1 + \epsilon_1 y_6)}. \tag{21}$$

RESULTS AND CONVERSATION

In this portion, we graphically analyze the behavior of dimensionless parameters on concentration, fluid velocity, and temperature dissemination. Furthermore, we describe the influence of non-dimensional parameters on physical characteristics of fluid such as skin friction and Nusselt and Sherwood numbers through tables.

Influence of α on velocity dissemination

The variation in α on velocity dissemination for definite values of m is shown in Fig. 2. We observe that the axial velocity component of f monotonically increases with the variable η if $0 \leq \alpha < 0.5$, but the component of velocity decreases with increase in η , whenever α is greater than 0.5. It can be seen that the axial component of velocity decreases at the barrier of the pin but increases when away from the pin, when α is greater than 0.5, but velocity dissemination behaves oppositely whenever $0 \leq \alpha < 0.5$. At $\alpha = 0.5$, we observe that velocity shows a constant behavior.

Influence of the visco-elastic parameter γ on velocity dissemination

Figure 3 depicts the impact of the viscoelastic parameter γ on velocity dissemination. The figure illustrates that fluid velocity dissemination and thickness of the momentum boundary layer declines

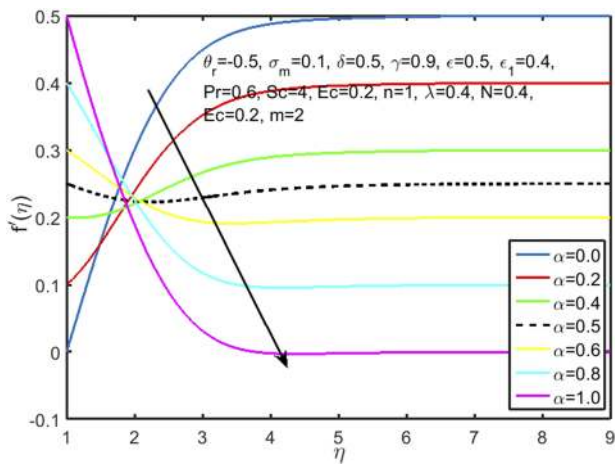


FIG. 2. Significance of α on $f'(\eta)$.

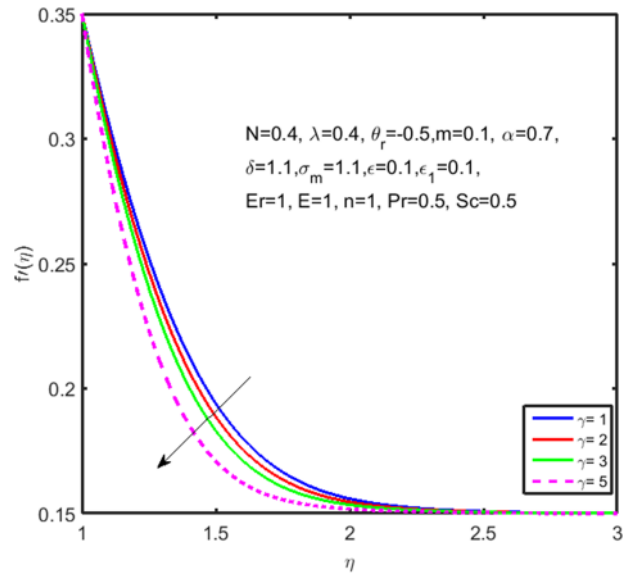


FIG. 3. Significance of γ on $f'(\eta)$.

for an amplified value of γ . Experimentally, it is observed that the parameter γ is directly related to the fluid viscosity and inversely related to the yield stress. Hence, these factors reduce the boundary layer thickness of hydrodynamics (momentum) and velocity of fluid.

Influence of λ on velocity dissemination

The mixed convection parameter λ is a ratio between buoyancy and inertial forces. The demeanor of this parameter on velocity dissemination is displayed in Fig. 4. It can be seen that for superior

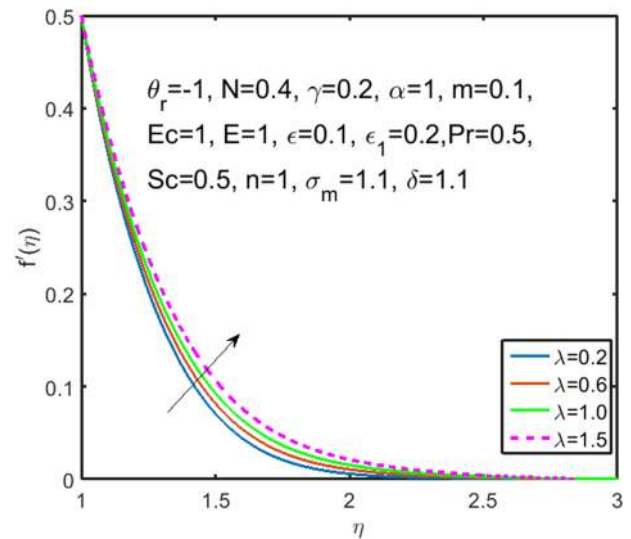


FIG. 4. Significance of λ on $f'(\eta)$.

values of the mixed convection parameter, both momentum and velocity boundary layer thickness increases. It is important to include that values of λ are either zero or non-zero depend on the nonexistence or existence of the mixed convection parameter. Moreover, positive values of λ identify that heat is convicted from the barrier of the pin to the fluid flow. It is observed that with the increase in λ , the inertial force decreases, where buoyancy force and $T_w - T_\infty$ increases. These circumstances increase the velocity of fluid.

Influence of the concentration buoyancy parameter N on velocity dissemination

Figure 5 clarifies the behavior of velocity dissemination for different values of the concentration buoyancy parameter N. We observe that superior values of the parameter N give a magnifying behavior of velocity dissemination.

Influence of θ_r on velocity dissemination

Figure 6 illustrates the graphical demeanor of velocity dissemination for different values of the viscosity parameter θ_r . We noted that the thickness of the velocity boundary layer and velocity dissemination condenses for higher values of the viscosity parameter. The reason is that resistance of the flow is inversely proportional to fluid velocity, and the amplification of fluid viscosity increases the resistance of the fluid which condenses the fluid velocity.

Influence of ϵ on temperature dissemination

The influence of the thermal conductivity parameter ϵ on non-dimensional temperature dissemination is displayed in Fig. 7. We observe that when thermal conductivity is constant, i.e., when $\epsilon = 0$, then fluid temperature is smaller than temperature of fluid when thermal conductivity is a variable. The thickness of the thermal boundary layer and temperature dissemination increases for large

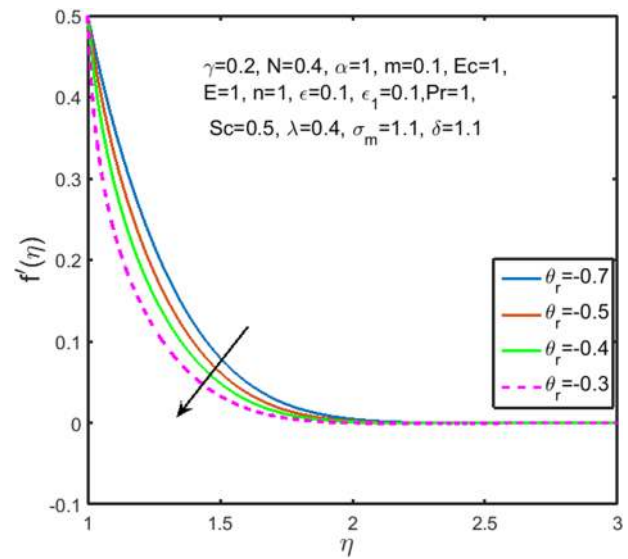


FIG. 6. Significance of θ_r on $f'(\eta)$.

values of ϵ . We see that the thermal boundary layer thickness of fluid is larger for varying thermal conductivity and smaller for constant thermal conductivity.

Influence of the Eckert number Ec on temperature dissemination

The demeanor of temperature dissemination for several values of the Eckert parameter Ec is presented in Fig. 8. It can be

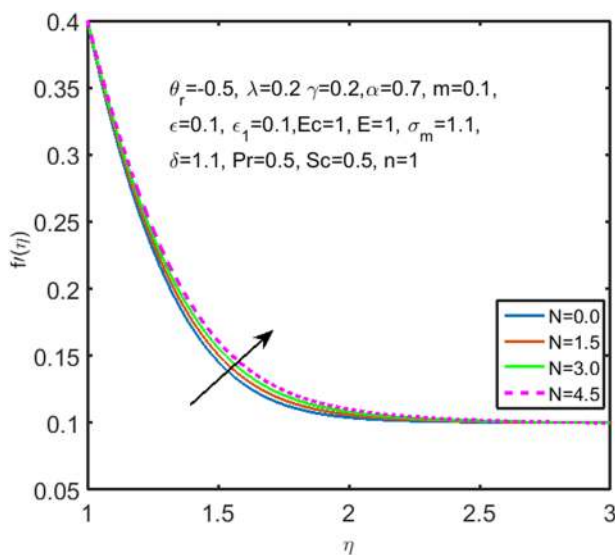


FIG. 5. Significance of N on $f_r(\eta)$.

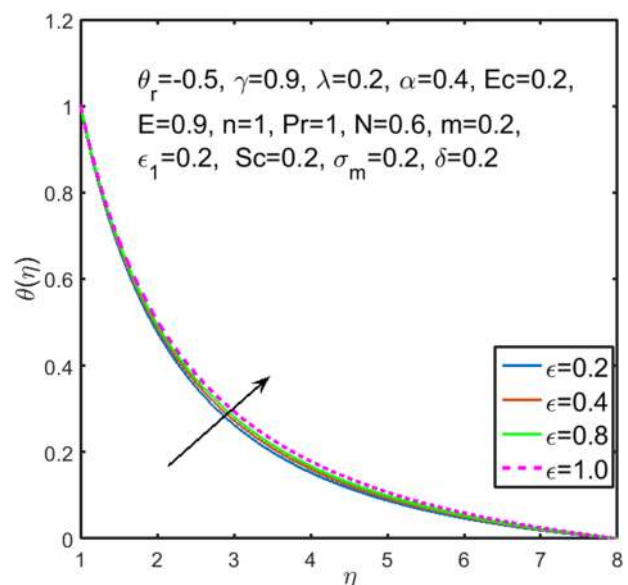


FIG. 7. Significance of ϵ on $\theta(\eta)$.

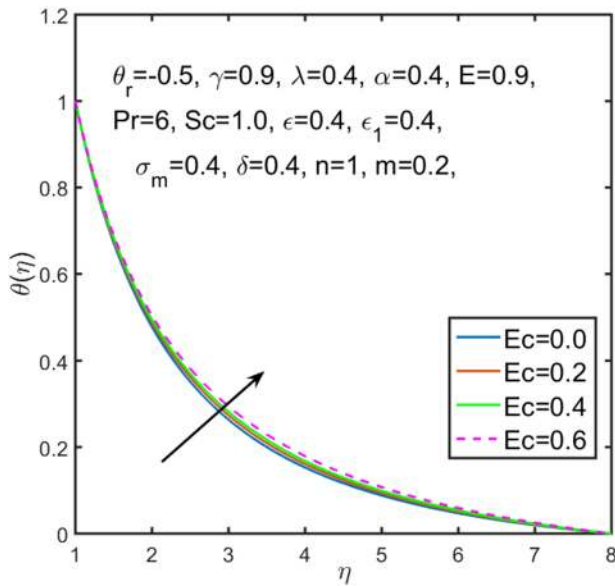


FIG. 8. Significance of Ec on $\theta(\eta)$.

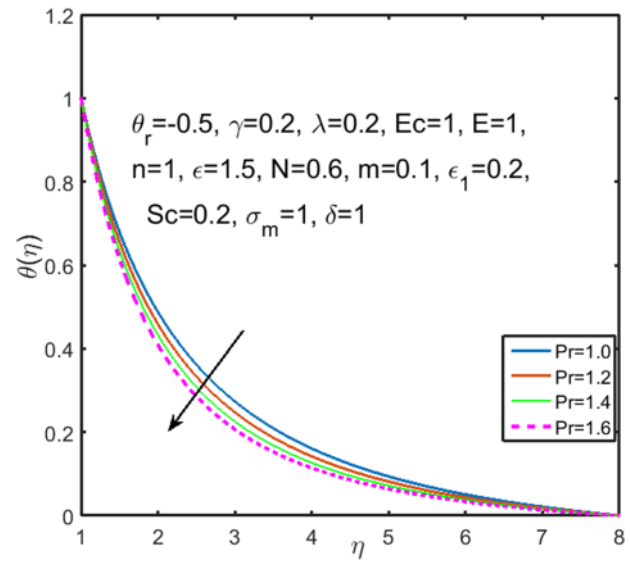


FIG. 9. Significance of Pr on $\theta(\eta)$.

seen that non-dimensional temperature significantly increases for mounting values of Ec . Since Ec appears as a coefficient of internal energy change, an increase in fluid temperature is understandable. Moreover, an increase in the Eckert number corresponds to a case: when heat is dissipated due to viscous force, this dissipated heat flows toward the fluid. Due to this fact, the temperature of the fluid increases. The figure shows that thermal boundary layer thickness enhances for superior values of the Eckert number. $Ec = 0$ corresponds to a case in which change in internal energy is insignificant. We observe that temperature of fluid is larger when change in internal energy is insignificant as compared to temperature of fluid in which change in internal energy is significant. Practically, for viscoelastic fluid flow, a negligible internal energy change is more suitable in controlling thermal boundary thickness.

Influence of the Prandtl number Pr on temperature dissemination

Dimensionless temperature dissemination for distinct values of Pr is displayed in Fig. 9. It has been observed that for an improving Prandtl number Pr , both temperature dissemination and thermal boundary layer thickness condense. Physically, the Prandtl number Pr is inversely proportional to thermal diffusivity, so an escalation in the Prandtl number is a cause of weedier thermal diffusion. Due to this fact, temperature dissemination reduces.

Influence of σ_m on concentration dissemination

The impact of the chemical reaction rate parameter σ_m for various values on concentration dissemination inside the boundary layer is demonstrated in Fig. 10. We noticed that if we improve the values of the chemical reaction rate parameter σ_m , we get a plummeting behavior in concentration dissemination inside the thermal

boundary layer expanse. The reason is that mounting the parameter σ_m causes condensing of the mass transfer boundary layer. This condensed value of mass reduces concentration dissemination.

Influence of ϵ_1 on concentration dissemination

Figure 11 shows the demeanor of concentration dissemination for various values of the mass diffusion coefficient ϵ_1 . We noted that dispersing species has a growing behavior for growing values of the

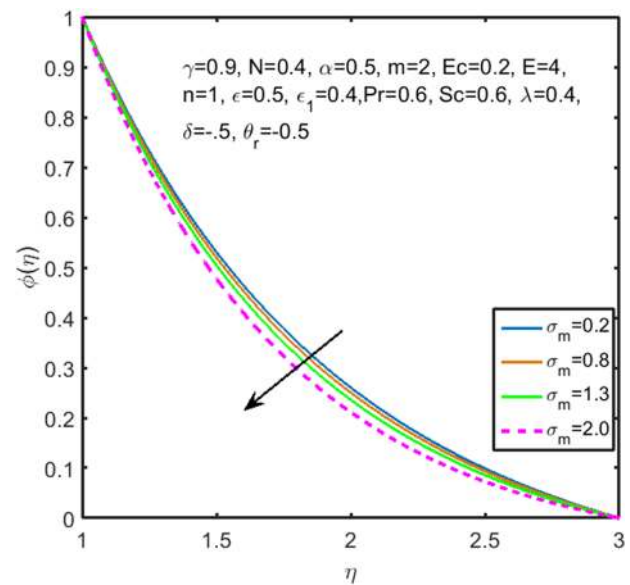


FIG. 10. Significance of σ_m on $\phi(\eta)$.

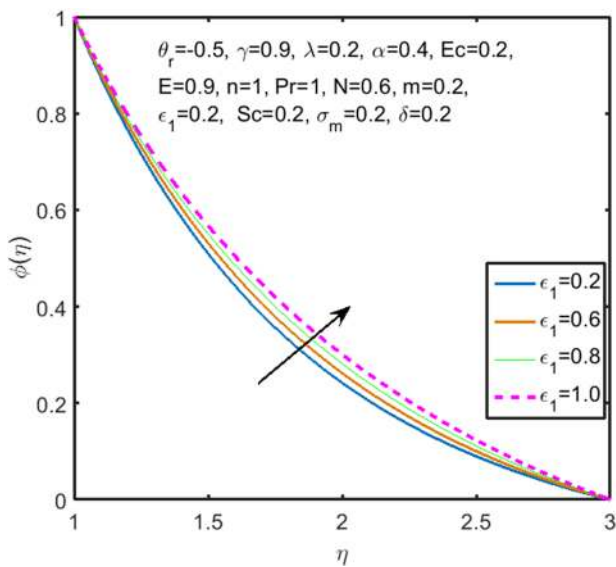


FIG. 11. Significance of ϵ_1 on $\phi(\eta)$.

diffusion coefficient ϵ_1 . Therefore, the thickness of the concentration boundary layer increases when ϵ_1 is enlarged.

Influence of the dimensionless energy activation parameter E on concentration dissemination

Figure 12 displays the impact of the dimensionless activation energy E on concentration dissemination. Generally, energy activation is the amount of energy that is used to stimulate atoms or molecules for chemical reaction. There should be a considerable number of atoms whose activation energy is less than or equal

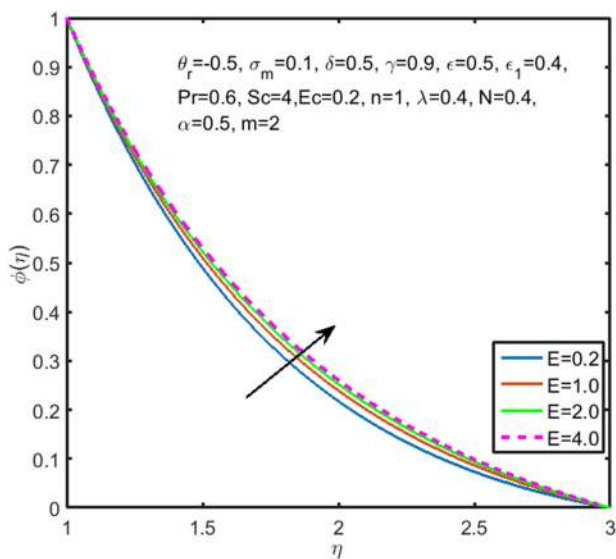


FIG. 12. Significance of E on $\phi(\eta)$.

to translational energy in a chemical reaction. We observe that solute layer thickness and concentration dissemination grow for mounting values of the parameter E . We examine that a greater value of the activation energy parameter E creates an increase in the term $\exp(\frac{-Ea}{kT})$, which leads to modification of concentration dissemination.

Influence of the Schmidt number Sc on concentration dissemination

The demeanor of concentration dissemination for several values of the parameter Sc is described in Fig. 13. The Schmidt number is the ratio between the diffusivity of hydrodynamics (momentum) and mass. Moreover, the Schmidt number Sc describes the comparative thickness of the concentration layer to the momentum layer. A higher Schmidt number Sc attributes to smaller mass diffusivity. Hence, the existence of Sc in the concentration equation considerably modifies the concentration dissemination regime. The figure indicates that concentration dissemination reduces for amplifying values of Sc .

Influence of the fitted rate constant n on concentration figure

The performance of concentration dissemination for miscellaneous values of the fitted rate constant n is labeled in Fig. 14. We observe that the factor $\sigma_m(1 + \theta\delta)^n \exp(\frac{-E}{1+\theta\delta})$ increases for increasing values of n . This factor creates destruction in the chemical reaction which elevates the fluid concentration.

Influence of the temperature difference parameter δ on concentration dissemination

We analyze the impact of the temperature difference parameter δ on concentration dissemination, shown in Fig. 15. We observe

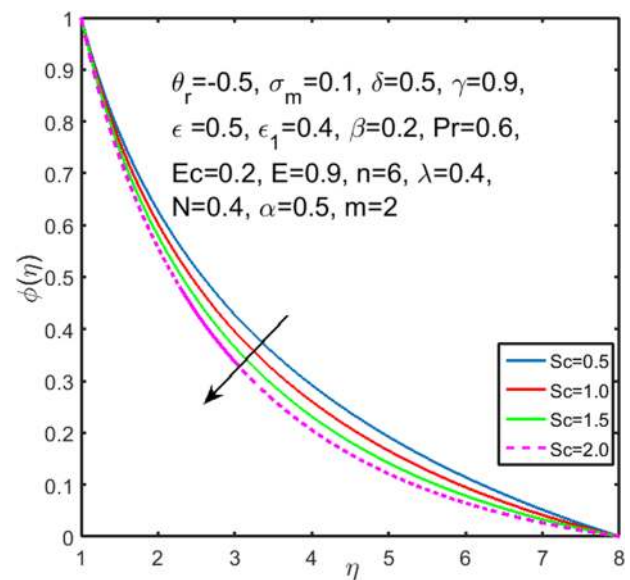


FIG. 13. Significance of Sc on $\phi(\eta)$.

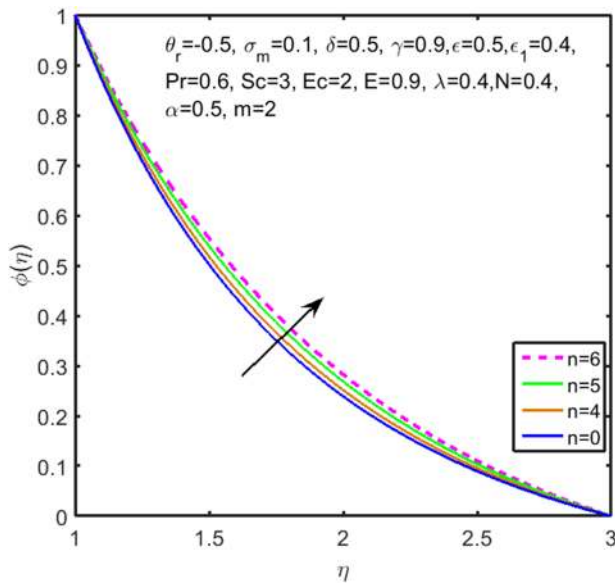


FIG. 14. Significance of n on $\phi(\eta)$.

that δ and solute concentration are inversely proportional to each other. The graph infers that concentration boundary layer thickness condenses when there exists a large difference between ambient temperature and surface temperature of the pin.

Demeanor of skin friction

Table I gives the numerical behaviors of the skin friction coefficient for different values of parameters λ , N , and θ_r . We observe that

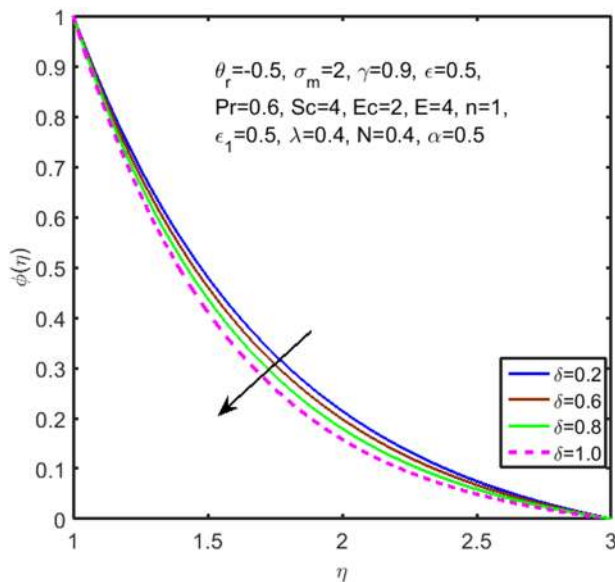


FIG. 15. Significance of δ on $\phi(\eta)$.

TABLE I. Skin friction coefficient for distinct values of λ , N , and θ_r when $m = 1.1$, $\alpha = 0.4$, $\gamma = \infty$, $\epsilon = 0.4$, $Pr = 1$, $E = 1.2$, $Ec = 0.7$, $\epsilon_1 = 0.4$, $Sc = 1$, and $\sigma_m = 0.6$.

N	λ	θ_r	$C_f Re_x^{\frac{1}{2}}$
0.2	0.4		-1.8973
0.6			-1.8257
1.0			-1.7632
1.2	0.4		-1.8973
	0.8		-1.6342
	1.2		-1.5421
	0.4	-1.0	-1.8973
		-0.7	-1.9681
		-0.4	-2.0356
		-0.1	-2.1428

the absolute value of the skin friction coefficient reduces for growing values of λ and N . However, skin friction shows an opposite behavior for increasing values of θ_r .

Demeanor of the Nusselt number

Table II demonstrates the performance of the local Nusselt number for miscellaneous values of non-dimensional parameters. The first three entries of the last column indicate that the local Nusselt number increases for higher values of the velocity ratio

TABLE II. Local Nusselt number for distinct values of θ_r , α , Pr , and γ when $m = 1.1$, $N = 0.4$, $\lambda = 0.2$, $\epsilon_1 = 0.2$, and $Sc = 1$.

α	ϵ	Pr	Ec	θ_r	γ	$Nu_x Re_x^{\frac{1}{2}}$
0.2						2.6835
0.3						2.7293
0.4						2.7506
0.2	0.2					2.6835
	0.7					2.4318
	1.2					2.3279
	1.7					2.1873
	0.2	0.6				2.6835
		1.0				2.8518
		1.4				2.8946
		1.7				2.9395
		0.6	0.2			2.6835
			0.4			2.6317
			0.6			2.5942
			0.8			2.5831
			0.2	-0.5		2.6835
				-0.4		2.5364
				-0.3		2.4122
				-0.2		2.1749
				-0.5	2	2.6835
					5	2.6671
					8	2.6347
					12	2.6136

TABLE III. Sherwood number for distinct values of α , σ_m , δ , Sc , E , ϵ_1 , and n when $m = 1.1$, $\gamma = \infty$, $\lambda = 0.4$, $\epsilon = 0.3$, $N = 0.4$ and $Pr = 1$, and $Ec = 1.5$.

α	σ_m	δ	Sc	n	ϵ_1	E	$Sh Re_x^{\frac{1}{2}}$
0.2							0.4946
0.4							0.4773
0.6							0.4682
0.2	0.8						0.5263
	1.2						0.5683
	1.6						0.5725
	0.4	0.8					0.5076
		1.2					0.5102
		1.6					0.5188
		0.4	1.0				0.5009
			1.4				0.5053
			1.8				0.5086
			0.6	2			0.5614
				3			0.6075
				4			0.6338
				1	0.4		0.4897
					0.6		0.4839
					0.8		0.4790
					0.1	1.0	0.4862
						1.5	0.4819
						2.0	0.4776

parameter α . In short, we can say that the local Nusselt number is linearly dependent on the velocity ratio parameter α . The table clarifies that the heat transfer rate decreases when the viscoelastic parameter γ is enlarged. We found that the Nusselt number also declines when the temperature difference parameter ϵ enhances. We also noticed that the Nusselt number condenses for rising values of the Eckert number Ec . The table infers that the local Nusselt number mounted for escalating values of Pr . The Nusselt number shows a mounting behavior for higher absolute values of θ_r .

Demeanor of the Sherwood number

The behavior of the Sherwood number for miscellaneous values of embedded parameters α , ϵ_1 , Sc , σ_m , δ , and E is illuminated in Table III. We found that the Sherwood number enhances when the velocity of the needle is larger than the velocity of the mainstream. We find an accumulating behavior of the Sherwood number for growing values of α , σ_m , δ , Sc , and n . However, we observe shrinkage in the behavior of the Sherwood number for higher values of ϵ_1 and E .

DEDUCTIVE REMARKS

We have performed the investigation on boundary layer flow over a continuously moving vertical pin in a viscoelastic fluid flow. This article is based on the assumptions of variable thermo-physical properties of fluid along with the pre-exponential factor and internal energy change. Extracted similarity equations are solved by the Matlab software (Bvp4c). The existing investigation enables us to draw the following remarks worth mentioning:

- Velocity dissemination increases when $0 \leq \alpha < 0.5$. However, velocity dissemination decreases when the ratio parameter is greater than 0.5. The velocity profile does not show any variation when $\alpha = 0.5$.
- Velocity dissemination falls for growing values of viscoelastic parameters γ , but in the case of the mixed convection parameter λ , we get an opposite behavior.
- Velocity dissemination enhances for improving values of N but declines for improving values of θ_r .
- Temperature dissemination expands for expending values of ϵ and Ec but declines for expending values of Pr and σ_m .
- The demeanor of fluid concentration amplifies for amplifying values of ϵ_1 and the non-dimensional activation energy parameter E .
- Concentration dissemination upswings for larger values of the fitted rate constant n .
- Fluid concentration shows a magnifying behavior for reducing values of Sc and δ .
- Absolute values of skin friction condenses for larger values of the buoyancy concentration parameter N and the mixed convection parameter λ but shows a conflicting behavior for large values of the variable thermal conductivity parameter θ_r .
- Numerical values of the local Nusselt number upswing if the values of the temperature difference parameter ϵ , viscosity parameter θ_r , Eckert number Ec , and viscoelastic parameter γ decrease but show an opposite behavior if the values of α and Pr increase.
- The Sherwood number enhances for higher values of σ_m , δ , Sc , and n but reduces for ϵ_1 , α , and E .

REFERENCES

- ¹P. M. Patil and P. S. Kulkarni, "Effects of chemical reaction on free convective flow of polar fluid through a porous medium in the presence of internal heat generation," *Int. J. Therm. Sci.* **47**, 1043–1054 (2008).
- ²T. Hayat, Z. Abbas, and M. Sajid, "Heat and mass transfer analysis on the flow of second grade fluid in presence of chemical reaction," *Phys. Lett. A* **372**, 2400–2408 (2008).
- ³Kh. A. Maleque, *Effects of Binary Chemical Reaction and Activation Energy on MHD Boundary Layer Heat and Mass Transfer Flow with Viscous Dissipation and Heat Generation/Absorption* (Hindawi Publishing Corporation, 2013).
- ⁴F. G. Awad, S. Motsa, and M. Khumalo, "Heat and mass transfer in unsteady rotating fluid flow with binary chemical reaction and activation energy," *PLoS One* **9**, e107622 (2014).
- ⁵Z. Shafique, A. Mustafa, and A. Mushtaq, "Boundary layer flow of Maxwell fluid in rotating frame with binary chemical reaction and activation energy," *Result Phys.* **6**, 627–633 (2016).
- ⁶K.-L. Hsiao, "To promote radiation electrical MHD activation energy thermal extrusion manufacturing system energy by using Carreau-Nanofluid with parameters control method," *Energy* **130**, 486 (2017).
- ⁷D.-C. Lu, M. Ramzan, M. Bilal, J. D. Chung, and U. Farooq, "A numerical investigation of 3D MHD rotating flow with binary chemical reaction, activation energy and non-Fourier heat flux," *Commun. Theor. Phys.* **70**, 89–96 (2018).
- ⁸A. Hamid, Hashim, and M. Khan, "Impacts of binary chemical reaction and activation energy on unsteady flow of magneto-Williamson nanofluid," *J. Mol. Liq.* **262**, 435–442 (2018).
- ⁹M. Dhlamini, P. K. Kameswaran, P. Sibanda, S. Motsa, and H. Mondal, "Activation energy and binary chemical reaction effects in mixed convective nanofluid flow with convective boundary condition," *J. Comput. Des. Eng.* **6**, 149 (2019).

- ¹⁰A. Majeed, F. M. Noorib, A. Zeeshan, T. Mahmood, S. U. Rehman, and I. Khan, "Analysis of activation energy in magnetohydrodynamic flow with chemical reaction and second order momentum slip model," *Case Stud. Therm. Eng.* **12**, 765–773 (2018).
- ¹¹M. I. Khan, S. Qayyum, T. Hayat, M. Waqas, M. I. Khan, and A. Alsaedi, "Entropy generation minimization and binary chemical reaction with Arrhenius activation energy in MHD radiative flow of nanomaterial," *J. Mol. Liq.* **259**, 274–283 (2018).
- ¹²M. Ijaz and M. Ayub, "Nonlinear convective stratified flow of Maxwell nanofluid with activation energy," *Heliyon* **5**, e01121 (2019).
- ¹³H. C. Brinkman, "Heat effects in capillary flow," *Appl. Sci.* **2**, 120–124 (1951).
- ¹⁴D. Wei and H. Luo, "Finite element solutions of heat transfer in molten polymer flow in tubes with viscous dissipation," *Int. J. Heat Mass Transfer* **46**, 3097–3108 (2003).
- ¹⁵O. Jambal, T. Shigechi, G. Davaa, and S. Momoki, "Effects of viscous dissipation and fluid axial heat conduction on heat transfer for non-Newtonian fluids in duct with uniform wall temperature," *Int. Commun. Heat Mass Transfer* **32**, 1165–1173 (2005).
- ¹⁶R. R. Kairi and P. V. S. N. Murthy, "Effect of viscous dissipation on natural convection heat and mass transfer from vertical cone in non-Newtonian fluid saturated non-Darcy porous medium," *Appl. Math. Comput.* **217**, 8100–8114 (2011).
- ¹⁷M. A. El-Aziz, "Unsteady mixed convection heat transfer along a vertical stretching surface with variable viscosity and viscous dissipation," *J. Egypt. Math. Soc.* **22**, 529–537 (2014).
- ¹⁸S. Saleem and S. Nadeem, "Theoretical analysis of slip flow on a rotating cone with viscous dissipation effects," *J. Hydrodyn.* **27**, 616–623 (2015).
- ¹⁹S. R. Sheri and Shamshuddin MD, "Heat and mass transfer on MHD flow of micropolar fluid in presence of viscous dissipation and chemical reaction," *Proc. Eng.* **127**, 885–892 (2015).
- ²⁰A. Hussain, M. Y. Malik, S. Bilal, M. Awais, and T. Salahuddin, "Computational analysis of magnetohydrodynamics Sisko fluid flow over a stretching cylinder in presence of viscous dissipation and temperature dependent thermal conductivity," *Results Phys.* **7**, 139–146 (2017).
- ²¹A. Hussain, M. Y. Malik, T. Salahuddin, A. Rubab, and M. Khan, "Effects of viscous dissipation on MHD tangent hyperbolic fluid over a nonlinear stretching sheet with convective boundary conditions," *Results Phys.* **7**, 3502–3509 (2017).
- ²²A. Hussain, M. Y. Malik, T. Salahuddin, S. Bilal, and M. Awais, "Combined effect of viscous dissipation and Joule heating on MHD Sisko nano-fluid over a stretching cylinder," *J. Mol. Liq.* **231**, 341–352 (2017).
- ²³E. M. E. Elbarbary and N. S. Elagzery, "Chebyshev finite difference method for the effects of variable viscosity and variable thermal conductivity on heat transfer on moving surfaces with radiation," *Int. J. Therm. Sci.* **43**, 889–899 (2004).
- ²⁴A. M. Saleem, "Variable viscosity and thermal conductivity effects on MHD flow and heat transfer in viscoelastic fluid over a stretching sheet," *Phys. Lett. A* **369**(4), 315–322 (2007).
- ²⁵N. Ahmad, Z. U. Siddiqui, and M. K. Mishra, "Boundary layer flow and heat transfer past a stretching surface with variable thermal conductivity," *Int. J. Nonlinear Mech.* **45**, 306–309 (2010).
- ²⁶T. Hayat, M. Ijaz Khan, M. Farooq, N. Gull, and A. Alsaedi, "Unsteady three dimensional mixed convection flow with variable viscosity and thermal conductivity," *J. Mol. Liq.* **223**, 1297–1310 (2016).
- ²⁷Hashim, A. Hamid, and M. Khan, "Unsteady mixed convection flow of Williamson nanofluid with heat transfer in the presence of variable thermal conductivity and magnetic field," *J. Mol. Liq.* **260**, 436–446 (2018).
- ²⁸A. Pantokratoras, "Study of MHD boundary layer flow over a heated stretching sheet with variable viscosity: A numerical reinvestigation," *Int. J. Heat Mass Transfer* **51**, 104–110 (2008).
- ²⁹R. Tsai, K. H. Huang, and J. S. Huang, "The effects of variable viscosity and thermal conductivity on heat transfer for hydromagnetic flow over a continuous moving porous plate with Ohmic heating," *Appl. Therm. Eng.* **29**, 1921–1926 (2009).
- ³⁰M. Y. Malik, A. Hussain, and S. Nadeem, "Boundary layer flow of an Eyring-Powell model fluid due to a stretching cylinder with variable viscosity," *Sci. Iran.* **20**, 313–321 (2013).
- ³¹M. Y. Malik, M. Khan, T. Salahuddin, and I. Khan, "Variable viscosity and MHD flow in Casson fluid with Christeano-Christov heat flux model, Using Keller box method," *Eng. Sci. Technol. Int. J.* **19**, 1985–1992 (2016).
- ³²J. C. Umavathi, M. A. Sheremet, and S. Mohiuddin, "Combined effect of variable viscosity and thermal conductivity on mixed convection flow of viscous fluid in a vertical channel in the presence of first order chemical reaction," *Eur. J. Mech. B: Fluids* **58**, 98–108 (2016).
- ³³T. E. Akinbobola and S. S. Okoya, "The flow of second grade fluid over a stretching sheet with variable thermal conductivity and viscosity in the presence of heat source/sink," *J. Niger. Math. Soc.* **34**, 331–342 (2015).
- ³⁴R. Muthucumaraswamy, "Effects of chemical reaction on moving isothermal vertical plate with variable mass diffusion," *Theor. Appl. Mech.* **3**, 209–220 (2003).
- ³⁵R. Muthucumaraswamy and B. Janakiraman, "MHD and radiation effects on moving isothermal vertical plate with variable mass diffusion," *Theor. Appl. Mech.* **1**, 17–29 (2006).
- ³⁶V. Rajesh and S. V. K. Varma, "Radiation effects on MHD flow through a porous medium with variable temperature and variable mass diffusion," *Int. J. Appl. Math. Mech.* **6**, 39–57 (2010).
- ³⁷X. Jia, F. Zeng, and Y. Gu, "Semi analytical solution to one-dimensional advection-diffusion equations with variable diffusion coefficient and variable flow velocity," *Appl. Math. Comput.* **221**, 268–281 (2013).
- ³⁸C. Li, H. Guo, and X. Tian, "Time-domain finite Element analysis to non-linear transient responses of generalized diffusion-thermoelasticity with variable thermal conductivity and diffusivity," *Int. J. Mech. Sci.* **131–132**, 234–244 (2017).
- ³⁹L.-T. Sheng, S.-L. Chiu, and S.-S. Hsiau, "Effect of mass diffusion upon thermal-diffusive of a dry vibrated granular bed," *Chem. Eng. Sci.* **185**, 222–230 (2018).
- ⁴⁰I. H. Qureshi, M. Nawaz, S. Rana, and T. Zubair, "Galerkin finite element study on the effects of variable thermal conductivity and variable mass diffusion conductance on heat and mass transfer," *Commun. Theor. Phys.* **70**, 49–59 (2018).
- ⁴¹M. Khan, T. Salahuddin, A. Tanveer, M. Y. Malik, and A. Hussain, "Change in internal energy of thermal diffusion stagnation point Maxwell nanofluid flow along with solar radiation and thermal conductivity," *Chin. J. Chem. Eng.* **27**, 2352 (2019).
- ⁴²Q. Xiong, I. Tlili, R. N. Dara, A. Shafee, T. Nguyen-Thoi, A. Rebey, R.-ul Haq, and Z. Li, "Energy storage simulation involving NEPCM solidification in appearance of fins," *Physica A* (published online).
- ⁴³N. Ullah, S. Nadeem, A. U. Khan, R. Ul Haq, and I. Tlili, "Influence of metallic nanoparticles in water driven along a wavy circular cylinder," *Chin. J. Phys.* **63**, 168–185 (2020).
- ⁴⁴A. Zaib, R. Ul Haq, M. Sheikholeslami, and U. Khan, "Numerical analysis of effective Prandtl model on mixed convection flow of $\gamma\text{Al}_2\text{O}_3\text{-H}_2\text{O}$ nanoliquids with micropolar liquid driven through wedge," *Phys. Scr.* (published online).
- ⁴⁵Z. H. Khan, O. D. Makinde, M. Hamid, R. U. Haq, and A. Khan, "Hydromagnetic flow of ferrofluid in an enclosed partially heated trapezoidal cavity filled with a porous medium," *J. Magn. Magn. Mater.* **499**, 166241 (2019).